

# A refined HSDT for bending and dynamic analysis of FGM plates

Fatima Zohra Zaoui<sup>\*1a</sup>, Abdelouahed Tounsi<sup>2,3</sup>, Djamel Ouinas<sup>1</sup> and Jaime A. Viña Olay<sup>4</sup>

<sup>1</sup>Laboratory of numerical and experimental modeling of the mechanical phenomena, Mechanical Engineering Department, Faculty of sciences and Technology / Ibn Badis University, 27000 Mostaganem, Algeria

<sup>2</sup>Material and Hydrology Laboratory, Civil Engineering Department, Faculty of Technology/ Djilali Liabes University, 22000 Sidi Bel Abbes, Algeria

<sup>3</sup>Department of Civil and Environmental Engineering, King Fahd University of Petroleum & Minerals, 31261 Dhahran, Eastern Province, Saudi Arabia

<sup>4</sup>Department of Materials Science and Metallurgical Engineering, Campus of Viesques, University of Oviedo, 33204 Gijón, Spain

(Received June 29, 2017, Revised October 5, 2017, Accepted November 27, 2019)

**Abstract.** In this work, a novel higher-order shear deformation theory (HSDT) for static and free vibration analysis of functionally graded (FG) plates is proposed. Unlike the conventional HSDTs, the proposed theory has a novel displacement field which includes undetermined integral terms and contains fewer unknowns. Equations of motion are obtained by using Hamilton's principle. Analytical solutions for the bending and dynamic investigation are determined for simply supported FG plates. The computed results are compared with 3D and quasi-3D solutions and those provided by other plate theories. Numerical results demonstrate that the proposed HSDT can achieve the same accuracy of the conventional HSDTs which have more number of variables.

**Keywords:** bending; vibration; functionally graded plate; shear deformation theory

## 1. Introduction

Functionally graded materials (FGMs) are fabricated from a mixture of two materials to accomplish a composition that produces a specific functionality. These materials are generally isotropic but nonhomogeneous. The reason for interest in FGMs is that it may be possible to provide certain kinds of FGM structures capable of adapting to operating conditions. Presenting novel characteristics, FGMs have also attracted intensive research interests, which were mainly focused on their bending, buckling, dynamic and vibration characteristics of FG structures (Akbaş, 2016, Eltaher *et al.* 2013, Ebrahimi *et al.* 2009a, b, Zaoui *et al.* 2017a, Guerroudj *et al.* 2018). Since the shear deformation has considerable influences on the responses of FG plates, shear deformation models are employed to capture such shear deformation influences. The first-order shear deformation theory (FSDT) considers the shear deformation influences by the way of linear distribution of in-plane displacements within the thickness (Mindlin, 1951, Meksi *et al.* 2015, Bouderba *et al.* 2016, Bellifa *et al.* 2016, Kolahchi *et al.* 2016a, b, Madani *et al.* 2016, Zamaniaan *et al.* 2017). Since the first-order shear deformation theory violates the conditions of zero transverse shear stresses on the upper and lower surfaces of the plate, a shear correction coefficient which is related to many parameters is required to compensate for the error due to a constant shear strain assumption within the thickness. The HSDTs consider the

shear deformation influences, and respect the zero transverse shear stresses on the upper and lower surfaces of the plate; hence, a shear correction coefficient is not needed. By employing HSDT, Mahapatra *et al.* (2017) studied nonlinear thermoelastic deflection of temperature-dependent FGM curved shallow shell under nonlinear thermal loading. Using the simple higher-order shear deformable kinematics including the temperature dependent properties of each constituent, Mehar and Panda (2017) studied the thermoelastic nonlinear frequency analysis of CNT reinforced FG sandwich structure. HSDTs are also used to study laminated composites structures with different loads cases (Kolahchi, 2017, Kolahchi *et al.* 2017a, b, Mahapatra *et al.* 2016a, b, c, d, e, Sahoo *et al.* 2016, Mahapatra and Panda, 2016, Mahapatra *et al.* 2015, Mahapatra and Panda, 2015, Kar *et al.* 2015). Kolahchi and Moniri Bidgoli (2016) used the sinusoidal shear deformation beam theory for dynamic instability of single-walled carbon nanotubes. Arani and Kolahchi employed HSDT to study buckling response of embedded concrete columns armed with carbon nanotubes. Bilouei *et al.* (2016) investigated the buckling of concrete columns retrofitted with Nano-Fiber Reinforced Polymer using HSDT.

In general, HSDTs are proposed based on the superposition of higher-order distributions of in-plane displacements (Reddy, 2000, Zenkour, 2006, Pradyumna and Bandyopadhyay, 2008, Ait Atmane *et al.* 2010, Benyoucef *et al.* 2011, Xiang *et al.* 2011, Bouderba *et al.* 2013, Thai and Kim, 2013, Tounsi *et al.* 2013, Ait Amar Meziane *et al.* 2014, Ait Yahia *et al.* 2015, Mahi *et al.* 2015, Kar *et al.* 2016a, b, Baseri *et al.* 2016, Beldjelili *et al.* 2016, Raminnea *et al.* 2016, Bousahla *et al.* 2016, Aldousari, 2017, Rahmani *et al.* 2017) or both axial and vertical displacements within the thickness (Matsunaga, 2008, Chen

\*Corresponding author, Ph.D. Student  
E-mail: fatima.zaoui@univ-mosta.dz,  
tima22000@hotmail.com

*et al.* 2009, Talha and Singh, 2010, Reddy, 2011, Neves *et al.* 2012a, b, Hebbali *et al.* 2014, Swaminathan and Naveenkumar, 2014, Bourada *et al.* 2015, Hamidi *et al.* 2015, Akavci, 2016, Bennoun *et al.* 2016). Some of these models are computational costs because with each additional power of the thickness coordinate, an additional variable is added to the theory (e.g., theories by Pradyumna and Bandyopadhyay (2008) and Neves *et al.* (2012a, b) with nine variables, Reddy (2011) with eleven unknowns, Talha and Singh (2010) with thirteen unknowns). Although some well-known HSDTs have the same five variables (e.g., third-order shear deformation theory (Reddy, 2000), sinusoidal shear deformation theory (Zenkour, 2006), hyperbolic shear deformation theory (Ait Atmane *et al.* 2010, Benyoucef *et al.* 2011)), their governing equations are much more complicated than those of FSDT. Thus, needs exist for the development of HSDTs which are simple to utilize.

The objective of this work is to construct a simple HSDT for FG plates. The proposed theory has only four variables and four equations of motion, but it respects the stress-free boundary conditions on the upper and lower surfaces of the plate without introducing any shear correction factors. The displacement field of the developed theory is chosen based on a constant vertical displacement and trigonometric variation of in-plane displacements within the thickness. The addition of the integral term into the in-plane displacements leads to a reduction in the number of variables and governing equations, hence makes the model simple to utilize. Analytical solutions for static and dynamic are obtained. Numerical examples are presented to check the accuracy of the proposed theory.

## 2. Theoretical formulation

### 2.1 Kinematics

The displacement field of the proposed theory is constructed based on the following suppositions: (1) the in-plane displacements are partitioned into bending and shear components; (2) the bending parts of the in-plane displacements are similar to those used by CPT; (3) the shear parts of the in-plane displacements are formulated by using the integral term and give rise to the trigonometric distributions of shear strains and hence to shear stresses within the thickness of the plate in such a way that the shear stresses vanish on the upper and lower surfaces of the plate; and (4) the transverse displacement is independent to the thickness coordinate. Based on these considerations, the following displacement field can be constructed

$$u(x, y, z, t) = u_0(x, y, t) - z \frac{\partial w_0}{\partial x} + k_1 f(z) \int \theta(x, y, t) dx \quad (1a)$$

$$v(x, y, z, t) = v_0(x, y, t) - z \frac{\partial w_0}{\partial y} + k_2 f(z) \int \theta(x, y, t) dy \quad (1b)$$

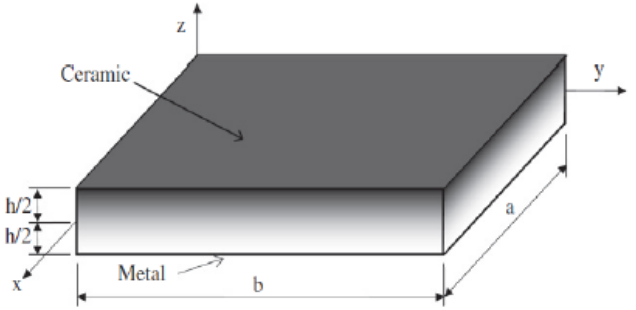


Fig. 1 Geometry and coordinates of FG plates

$$w(x, y, z, t) = w_0(x, y, t) \quad (1c)$$

where  $u_0(x, y, t)$ ,  $v_0(x, y, t)$ ,  $w_0(x, y, t)$  and  $\theta(x, y, t)$  are the four variables displacement functions of middle surface of the plate. Note that the integrals do not have limits. In the present study, it is employed terms with integrals instead of terms with derivatives. The constants  $k_1$  and  $k_2$  depends on the geometry.

In this work, the present HSDT is obtained by setting:

- Model 1

$$f(z) = \frac{h}{\pi} \sin\left(\frac{\pi z}{h}\right) \quad (2a)$$

- Model 2

$$f(z) = \frac{z}{2\pi} \left( \pi + 2 \cos \frac{\pi z}{h} \right) \quad (2b)$$

It should be noted that unlike the FSDT, this model does not require shear correction coefficients. The kinematic relations can be obtained as follows:

$$\begin{Bmatrix} \varepsilon_x \\ \varepsilon_y \\ \gamma_{xy} \end{Bmatrix} = \begin{Bmatrix} \varepsilon_x^0 \\ \varepsilon_y^0 \\ \gamma_{xy}^0 \end{Bmatrix} + z \begin{Bmatrix} k_x^b \\ k_y^b \\ k_{xy}^b \end{Bmatrix} + f(z) \begin{Bmatrix} k_x^s \\ k_y^s \\ k_{xy}^s \end{Bmatrix}, \quad (3a)$$

$$\begin{Bmatrix} \gamma_{yz} \\ \gamma_{xz} \end{Bmatrix} = g(z) \begin{Bmatrix} \gamma_{yz}^0 \\ \gamma_{xz}^0 \end{Bmatrix} \quad (3b)$$

Where

$$\begin{Bmatrix} \varepsilon_x^0 \\ \varepsilon_y^0 \\ \gamma_{xy}^0 \end{Bmatrix} = \begin{Bmatrix} \frac{\partial u_0}{\partial x} \\ \frac{\partial v_0}{\partial y} \\ \frac{\partial u_0}{\partial y} + \frac{\partial v_0}{\partial x} \end{Bmatrix}, \quad \begin{Bmatrix} k_x^b \\ k_y^b \\ k_{xy}^b \end{Bmatrix} = \begin{Bmatrix} -\frac{\partial^2 w_0}{\partial x^2} \\ -\frac{\partial^2 w_0}{\partial y^2} \\ -2 \frac{\partial^2 w_0}{\partial x \partial y} \end{Bmatrix}, \quad (4a)$$

$$\begin{Bmatrix} k_x^s \\ k_y^s \\ k_{xy}^s \end{Bmatrix} = \begin{Bmatrix} k_1 \theta \\ k_2 \theta \\ k_1 \frac{\partial}{\partial y} \int \theta dx + k_2 \frac{\partial}{\partial x} \int \theta dy \end{Bmatrix}, \quad (4b)$$

Table 1 Material properties employed in the FG plates

Properties	Ceramic		
	Metal Aluminum (Al)	Alumina (Al <sub>2</sub> O <sub>3</sub> )	Zirconia (ZrO <sub>2</sub> )
E(Gpa)	70	380	200
$\nu$	0.3	0.3	0.3
$\rho$ (kg/m <sup>3</sup> )	2702	3800	5700

$$\begin{Bmatrix} \gamma_{yz}^0 \\ \gamma_{xz}^0 \end{Bmatrix} = \begin{Bmatrix} k_2 \int \theta dy \\ k_1 \int \theta dx \end{Bmatrix}, \quad g(z) = \frac{df(z)}{dz} \quad (4c)$$

The integrals defined in the above equations shall be resolved by a Navier type method and can be written as follows:

$$\frac{\partial}{\partial y} \int \theta dx = A' \frac{\partial^2 \theta}{\partial x \partial y}, \quad \frac{\partial}{\partial x} \int \theta dy = B' \frac{\partial^2 \theta}{\partial x \partial y} \quad (5a)$$

$$\int \theta dx = A' \frac{\partial \theta}{\partial x}, \quad \int \theta dy = B' \frac{\partial \theta}{\partial y} \quad (5b)$$

where the coefficients  $A'$  and  $B'$  are expressed according to the type of solution employed, in this case via Navier. Therefore,  $A'$ ,  $B'$ ,  $k_1$  and  $k_2$  are expressed as follows:

$$A' = -\frac{1}{\alpha^2}, \quad B' = -\frac{1}{\beta^2}, \quad k_1 = \alpha^2, \quad k_2 = \beta^2 \quad (6)$$

where  $\alpha$  and  $\beta$  are defined in eq. (22).

## 2.2 Constitutive relations

The material characteristics of FG plates are considered to change continuously within the thickness. Three homogenization procedures employed to compute the Young's modulus  $E(z)$  are: (1) the power law variation, (2) the exponential variation, and (3) the Mori-Tanaka scheme.

For the power law variation, the Young's modulus is expressed as (Reddy 2000, Birman and Byrd 2007, Zidi *et al.* 2014, Zemri *et al.* 2015, Zidi *et al.* 2017)

$$E(z) = E_m + (E_c - E_m) \left( \frac{1}{2} + \frac{z}{h} \right)^p \quad (7a)$$

where  $p$  is the gradient index; and the subscripts  $m$  and  $c$  represent the metallic and ceramic constituents, respectively.

For the exponential variation, the Young's modulus is written as (Belabed *et al.* 2014, Meradjah *et al.* 2018)

$$E(z) = E_0 e^{p(z/h+1/2)} \quad (7b)$$

where  $E_0$  is the Young's modulus of the homogeneous plate; and  $p$  is a parameter that indicates the material distribution across the thickness of the plate.

For Mori-Tanaka scheme, the Young's modulus is defined as (Benveniste 1987, Mori and Tanaka 1973, Younsi *et al.* 2018)

$$E(z) = E_m + (E_c - E_m) \frac{V_c}{1 + (1 - V_c) \left( \frac{E_c}{E_m} - 1 \right) \frac{1 + \nu}{3 - 3\nu}} \quad (7c)$$

where  $V_c = (0.5 + z/h)^p$  is the volume fraction of the ceramic. Since the influences of the variation of Poisson's ratio  $\nu$  on the response of FG plates are very small (Yang *et al.* 2005, Kitipornchai *et al.* 2006), it is supposed to be constant for convenience.

The linear constitutive relations of an FG plate can be expressed as

$$\begin{Bmatrix} \sigma_x \\ \sigma_y \\ \tau_{yz} \\ \tau_{xz} \\ \tau_{xy} \end{Bmatrix} = \begin{bmatrix} Q_{11} & Q_{12} & 0 & 0 & 0 \\ Q_{12} & Q_{22} & 0 & 0 & 0 \\ 0 & 0 & Q_{44} & 0 & 0 \\ 0 & 0 & 0 & Q_{55} & 0 \\ 0 & 0 & 0 & 0 & Q_{66} \end{bmatrix} \begin{Bmatrix} \varepsilon_x \\ \varepsilon_y \\ \gamma_{yz} \\ \gamma_{xz} \\ \gamma_{xy} \end{Bmatrix} \quad (8)$$

where

$$\begin{aligned} Q_{11}(z) &= Q_{22}(z) = \frac{E(z)}{1 - \nu^2}, & Q_{12}(z) &= \nu Q_{11}(z) \\ Q_{44}(z) &= Q_{55}(z) = Q_{66}(z) = \frac{E(z)}{2(1 + \nu)} \end{aligned} \quad (9)$$

## 2.3 Equations of motion

Equations of motion are employed herein using Hamilton's principle (Zaoui *et al.* 2019, Chaabane *et al.* 2019). The principle can be stated in an analytical form as

$$\int_0^T (\delta U + \delta V - \delta K) dt = 0 \quad (10)$$

where  $\delta U$  is the variation of strain energy;  $\delta V$  is the variation of the external work done by external load applied to the FG plate; and  $\delta K$  is the variation of kinetic energy.

The variation of strain energy of the plate is given by

$$\begin{aligned} \delta U &= \int_V [\sigma_x \varepsilon_x + \sigma_y \varepsilon_y + \tau_{xy} \gamma_{xy} + \tau_{yz} \gamma_{yz} + \tau_{xz} \gamma_{xz}] dV \\ &= \int_A [N_x \delta \varepsilon_x^0 + N_y \delta \varepsilon_y^0 + N_{xy} \delta \gamma_{xy}^0 + M_x^b \delta k_x^b \\ &\quad + M_y^b \delta k_y^b + M_{xy}^b \delta k_{xy}^b + M_x^s \delta k_x^s + M_y^s \delta k_y^s \\ &\quad + M_{xy}^s \delta k_{xy}^s + S_{yz}^s \delta \gamma_{yz}^s + S_{xz}^s \delta \gamma_{xz}^0] dA \end{aligned} \quad (11)$$

Where  $A$  is the top surface and the stress resultants  $N$ ,  $M$  and  $S$  are defined by

$$\begin{aligned} (N_i, M_i^b, M_i^s) &= \int_{-h/2}^{h/2} (1, z, f) \sigma_i dz, \quad (i = x, y, xy) \\ (S_{xz}^s, S_{yz}^s) &= \int_{-h/2}^{h/2} g(z) (\tau_{xz}, \tau_{yz}) dz \end{aligned} \quad (12)$$

The variation of work done by external forces can be expressed as

$$\delta V = - \int_0^L q \delta w_0 dx \quad (13)$$

where  $q$  is the transverse load.

The variation of kinetic energy of the plate can be given as

$$\begin{aligned} \delta K &= \int_V (\dot{u} \delta \dot{u} + \dot{v} \delta \dot{v} + \dot{w} \delta \dot{w}) \rho(z) dV \\ &= \int_A \{ I_0 (\dot{u} \delta \dot{u} + \dot{v} \delta \dot{v} + \dot{w} \delta \dot{w}) \\ &\quad - I_1 \left( \dot{u}_0 \frac{\partial \delta \dot{w}_0}{\partial x} + \frac{\partial \dot{w}_0}{\partial x} \delta \dot{u}_0 + \dot{v} \frac{\partial \delta \dot{w}_0}{\partial y} + \frac{\partial \dot{w}_0}{\partial y} \delta \dot{v}_0 \right) \\ &\quad - I_2 \left( \frac{\partial \dot{w}_0}{\partial x} \frac{\partial \delta \dot{w}_0}{\partial x} + \frac{\partial \dot{w}_0}{\partial y} \frac{\partial \delta \dot{w}_0}{\partial y} \right) + K_2 \left( \frac{\partial \dot{\phi}}{\partial x} \frac{\partial \delta \dot{\phi}}{\partial x} + \frac{\partial \dot{\phi}}{\partial y} \frac{\partial \delta \dot{\phi}}{\partial y} \right) \\ &\quad - J_1 \left( \dot{u}_0 \frac{\partial \delta \dot{\phi}}{\partial x} + \frac{\partial \dot{\phi}}{\partial x} \delta \dot{u}_0 + \dot{v}_0 \frac{\partial \delta \dot{\phi}}{\partial y} + \frac{\partial \dot{\phi}}{\partial y} \delta \dot{v}_0 \right) \\ &\quad + J_2 \left( \frac{\partial \dot{w}_0}{\partial x} \frac{\partial \delta \dot{\phi}}{\partial x} + \frac{\partial \dot{\phi}}{\partial x} \frac{\partial \delta \dot{w}_0}{\partial x} + \frac{\partial \dot{w}_0}{\partial y} \frac{\partial \delta \dot{\phi}}{\partial y} + \frac{\partial \dot{\phi}}{\partial y} \frac{\partial \delta \dot{w}_0}{\partial y} \right) \} dA \end{aligned} \quad (14)$$

where dot-superscript convention represents the differentiation with respect to the time variable  $t$ ,  $\rho(z)$  is the mass density and the moments of inertia ( $I_i, J_i, K_i$ ) are expressed by

$$(I_0, I_1, I_2) = \int_{-h/2}^{h/2} \rho(z) [1, z, z^2] dz \quad (15a)$$

$$(J_1, J_2, K_2) = \int_{-h/2}^{h/2} \rho(z) [f, z f, f^2] dz \quad (15b)$$

Substituting the relations  $\delta U$ ,  $\delta V$  and  $\delta K$  from Eqs. (11), (13) and (14) into Eq. (10), integrating by parts and collecting the coefficients of  $\delta u_0$ ,  $\delta v_0$ ,  $\delta w_0$ ,  $\delta \theta$ , one obtains the following equations of motion

$$\delta u_0 : \frac{N_x}{\partial x} + \frac{N_{xy}}{\partial y} = I_0 \ddot{u}_0 - I_1 \frac{\partial \ddot{w}_0}{\partial x} + k_1 A' J_1 \frac{\partial \ddot{\phi}}{\partial x} \quad (16a)$$

$$\delta v_0 : \frac{N_{xy}}{\partial x} + \frac{N_y}{\partial y} = I_0 \ddot{v}_0 - I_1 \frac{\partial \ddot{w}_0}{\partial y} + k_2 B' J_1 \frac{\partial \ddot{\phi}}{\partial y} \quad (16b)$$

$$\begin{aligned} \delta w_0 : & \frac{\partial^2 M_x^b}{\partial x^2} + 2 \frac{\partial^2 M_{xy}^b}{\partial x \partial y} + \frac{\partial^2 M_y^b}{\partial y^2} + q \\ &= I_0 \ddot{w}_0 + I_1 \left( \frac{\partial \ddot{u}_0}{\partial x} + \frac{\partial \ddot{v}_0}{\partial y} \right) - I_2 \nabla^2 \ddot{w}_0 - J_2 \nabla^2 \ddot{\theta} \end{aligned} \quad (16c)$$

$$\begin{aligned} \delta \theta : & -k_1 M_x^s - k_2 M_y^s - (k_1 A' + k_2 B') \frac{\partial^2 M_{xy}^s}{\partial x \partial y} + k_1 A' \frac{\partial S_{xz}^s}{\partial x} + k_2 B' \frac{\partial S_{yz}^s}{\partial y} \\ &= -J_1 \left( k_1 A' \frac{\partial \ddot{u}_0}{\partial x} + k_2 B' \frac{\partial \ddot{v}_0}{\partial y} \right) - J_2 \left( k_1 A' \frac{\partial^2 \ddot{w}_0}{\partial^2 x} + k_2 B' \frac{\partial^2 \ddot{w}_0}{\partial^2 y} \right) \\ &\quad - K_2 \left( (k_1 A')^2 \frac{\partial^2 \ddot{\theta}}{\partial^2 x} + (k_2 B')^2 \frac{\partial^2 \ddot{\theta}}{\partial^2 y} \right) \end{aligned} \quad (16d)$$

Substituting Eq. (8) into Eq. (12) and integrating within the thickness of the plate, the stress resultants are expressed as

$$\begin{bmatrix} N_x \\ N_y \\ N_{xy} \\ M_x^b \\ M_y^b \\ M_{xy}^b \\ M_x^s \\ M_y^s \\ M_{xy}^s \end{bmatrix} = \begin{bmatrix} A_{11} & A_{12} & 0 \\ A_{12} & A_{22} & 0 \\ 0 & 0 & A_{66} \\ B_{11} & B_{12} & 0 \\ B_{12} & B_{22} & 0 \\ 0 & 0 & B_{66} \\ D_{11} & D_{12} & 0 \\ D_{12} & D_{22} & 0 \\ 0 & 0 & D_{66} \\ D_{11}^s & D_{12}^s & 0 \\ D_{12}^s & D_{22}^s & 0 \\ H_{11}^s & H_{12}^s & 0 \\ H_{12}^s & H_{22}^s & 0 \\ 0 & 0 & D_{66}^s \end{bmatrix} \begin{bmatrix} \epsilon_x^0 \\ \epsilon_y^0 \\ \gamma_{xy}^0 \\ k_x^b \\ k_y^b \\ k_{xy}^b \\ k_x^s \\ k_y^s \\ k_{xy}^s \end{bmatrix} \quad (17a)$$

$$\begin{bmatrix} S_{yz}^s \\ S_{xz}^s \end{bmatrix} = \begin{bmatrix} A_{44}^s & 0 \\ 0 & A_{55}^s \end{bmatrix} \begin{bmatrix} \gamma_{yz}^0 \\ \gamma_{xz}^0 \end{bmatrix} \quad (17b)$$

and stiffness components are expressed as

$$(A_{ij}, B_{ij}, D_{ij}, B_{ij}^s, D_{ij}^s, H_{ij}^s) = \int_{-h/2}^{h/2} [l, z, z^2, f(z), zf(z), f^2(z)] Q_{ij}(z) dz \quad (18a)$$

$$(i, j) = (1, 2, 6)$$

$$A_{44}^s = A_{55}^s = \int_{-h/2}^{h/2} [g(z)]^2 Q_{44}(z) dz \quad (18b)$$

## 2.4 Equations of motion in terms of displacements

By substituting Eq. (17) into Eq. (16), the equations of motion can be expressed in terms of displacements ( $u_0, v_0, w_0, \theta$ ) as

$$\begin{aligned} \delta u_0 : & A_{11} d_{11} u_0 + A_{66} d_{22} u_0 + (A_{12} + A_{66}) d_{12} v_0 \\ & - B_{11} d_{111} w_0 - (B_{12} + 2B_{66}) d_{122} w_0 + (k_1 B_{11}^s + k_2 B_{12}^s) d_1 \theta \\ & + (k_1 A' + k_2 B') B_{66}^s d_{122} \theta = I_0 \ddot{u}_0 - I_1 d_1 \ddot{w}_0 + (k_1 A') J_1 d_1 \ddot{\theta} \end{aligned} \quad (19a)$$

$$\begin{aligned} \delta v_0 : & (A_{12} + A_{66}) d_{12} u_0 + A_{66} d_{11} v_0 + A_{22} d_{22} v_0 \\ & - (B_{12} + 2B_{66}) d_{112} w_0 - B_{22} d_{222} w_0 + (k_1 B_{12}^s + k_2 B_{22}^s) d_2 \theta \\ & + (k_1 A' + k_2 B') B_{66}^s d_{112} \theta = I_0 \ddot{v}_0 - I_1 d_2 \ddot{w}_0 + (k_2 B') J_2 d_2 \ddot{\theta} \end{aligned} \quad (19b)$$

$$\begin{aligned} \delta w_0 : & B_{11} d_{11} \mu_0 + (B_{12} + 2B_{66}) d_{12} \mu_0 + (B_{12} + 2B_{66}) d_{112} v_0 \\ & + B_{22} d_{222} v_0 - D_{11} d_{111} w_0 - D_{22} d_{222} w_0 - 2(D_{12} + 2D_{66}) d_{1122} w_0 \\ & + (k_1 D_{11}^s + k_2 D_{12}^s) d_1 \theta + (k_1 D_{12}^s + k_2 D_{22}^s) d_2 \theta + 2(k_1 A' + k_2 B') D_{66}^s \\ & d_{1122} \theta + q = I_0 \ddot{w}_0 + J_0 \ddot{\theta} + I_1 (d_1 \ddot{u}_0 + d_2 \ddot{v}_0) - I_2 \nabla^2 \ddot{w}_0 + (k_1 A') J_2 d_1 \ddot{\theta} \\ & + (k_2 B') J_2 d_2 \ddot{\theta} \end{aligned} \quad (19c)$$

$$\begin{aligned} \delta \theta : & - (k_1 B_{11}^s + k_2 B_{12}^s) d_1 u_0 - (k_1 B_{12}^s + k_2 B_{22}^s) d_2 v_0 \\ & - B_{66}^s (k_1 A' + k_2 B') (d_{122} u_0 + d_{112} v_0) + (k_1 D_{11}^s + k_2 D_{12}^s) d_{11} w_0 \\ & + (k_1 D_{12}^s + k_2 D_{22}^s) d_{22} w_0 + 2D_{66}^s (k_1 A' + k_2 B') d_{1122} w_0 \\ & - (k_1^2 H_{11}^s + k_2^2 H_{22}^s + 2k_1 k_2 H_{12}^s) \theta + (k_1 A')^2 A_{55}^s d_{11} \theta \\ & + (k_2 B')^2 A_{44}^s d_{22} \theta - H_{66}^s (k_1 A' + k_2 B')^2 d_{1122} \theta \\ & = - J_1 (k_1 A' d_1 \ddot{u}_0 + k_2 B' d_2 \ddot{v}_0) + J_2 (k_1 A' d_{11} \ddot{w}_0 + k_2 B' d_{22} \ddot{w}_0) \\ & - K_2 ((k_1 A')^2 d_{11} \ddot{\theta} + (k_2 B')^2 d_{22} \ddot{\theta}) \end{aligned} \quad (19d)$$

Table 2 Non-dimensional stress and deflection of Al<sub>2</sub>/AlO<sub>3</sub> square plates

<i>p</i>	Theory	$\bar{\sigma}_x(h/3)$			$\bar{w}$		
		<i>a/h</i> = 4	<i>a/h</i> = 10	<i>a/h</i> = 100	<i>a/h</i> = 4	<i>a/h</i> = 10	<i>a/h</i> = 100
1	Quasi-3D (Neves <i>et al.</i> 2012a)	0.5925	1.4945	14.9690	0.6997	0.5845	0.5624
	Quasi-3D (Neves <i>et al.</i> 2012b)	0.5910	1.4917	14.9440	0.7020	0.5868	0.5648
	Quasi-3D (Neves <i>et al.</i> 2013)	0.5911	1.4917	14.9450	0.7020	0.5868	0.5647
	Quasi-3D (Carrera <i>et al.</i> 2008)	0.6221	1.5064	14.9690	0.7171	0.5875	0.5625
	Quasi-3D (Carrera <i>et al.</i> 2011)	0.6221	1.5064	14.9690	0.7171	0.5875	0.5625
	TSDT (Thai and Kim, 2013)	0.5812	1.4808	14.9676	0.7284	0.589	0.5625
	CPT	0.8060	2.0150	20.1500	0.5623	0.5623	0.5623
	FSDT	0.8060	2.0150	20.1500	0.7291	0.5889	0.5625
	Model 1	0.5796	1.4891	14.9675	0.7272	0.5888	0.5625
	Model 2	0.5803	1.4894	14.9675	0.7280	0.5889	0.5625
4	Quasi-3D (Neves <i>et al.</i> 2012a)	0.4404	1.1783	11.9320	1.1178	0.8750	0.8286
	Quasi-3D (Neves <i>et al.</i> 2012b)	0.4340	1.1593	11.7380	1.1095	0.8698	0.8241
	Quasi-3D (Neves <i>et al.</i> 2013)	0.4330	1.1588	11.7370	1.1108	0.8700	0.8240
	Quasi-3D (Carrera <i>et al.</i> 2008)	0.4877	1.1971	11.9230	1.1585	0.8821	0.8286
	Quasi-3D (Carrera <i>et al.</i> 2011)	0.4877	1.1971	11.9230	1.1585	0.8821	0.8286
	TSDT (Thai and Kim, 2013)	0.4449	1.1794	11.9209	1.1599	0.8815	0.8287
	CPT	0.6420	1.6049	16.0490	0.8281	0.8281	0.8281
	FSDT	0.6420	1.6049	16.0490	1.1125	0.8736	0.8286
	Model 1	0.4402	1.1774	11.9207	1.1626	0.882	0.8287
	Model 2	0.4424	1.1783	11.9208	1.1619	0.8818	0.8287
10	Quasi-3D (Neves <i>et al.</i> 2012a)	0.3227	1.1783	11.9320	1.3490	0.8750	0.8286
	Quasi-3D (Neves <i>et al.</i> 2012b)	0.3108	0.8467	8.6013	1.3327	0.9886	0.9228
	Quasi-3D (Neves <i>et al.</i> 2013)	0.3097	0.8462	8.6010	1.3334	0.9888	0.9227
	Quasi-3D (Carrera <i>et al.</i> 2008)	0.3695	0.8965	8.6077	1.3745	1.0072	0.9361
	Quasi-3D (Carrera <i>et al.</i> 2011)	0.3695	0.8965	8.6077	1.3745	1.0072	0.9361
	TSDT (Thai and Kim, 2013)	0.3259	0.8785	8.906	1.3909	1.0087	0.9362
	CPT	0.4796	1.1990	11.9900	0.9354	0.9354	0.9354
	FSDT	0.4796	1.1990	11.9900	1.3178	0.9966	0.9360
	Model 1	0.3214	0.8767	8.9058	1.3909	1.0089	0.9362
	Model 2	0.3235	0.8775	8.9059	1.3917	1.0089	0.9362

where  $dij$ ,  $dijl$  and  $dijlm$  are the following differential operators

$$d_i = \frac{\partial}{\partial x_i}, \quad d_{ij} = \frac{\partial^2}{\partial x_i \partial x_j}, \quad d_{ijl} = \frac{\partial^3}{\partial x_i \partial x_j \partial x_l}, \quad (20)$$

$$\partial_{ijlm} = \frac{\partial^4}{\partial x_i \partial x_j \partial x_l \partial x_m} \quad (i, j, l, m = 1, 2)$$

### 3. Analytical solutions

Consider a simply supported rectangular FG plate with length  $a$  and width  $b$  under transverse load  $q$  as shown in Fig. 1. Based on the Navier approach, the solutions are considered as

$$\begin{Bmatrix} u_0 \\ v_0 \\ w_0 \\ \theta \end{Bmatrix} = \sum_{m=1}^{\infty} \sum_{n=1}^{\infty} \begin{Bmatrix} U_{mn} e^{i\omega t} \cos(\alpha x) \sin(\beta y) \\ V_{mn} e^{i\omega t} \sin(\alpha x) \cos(\beta y) \\ W_{mn} e^{i\omega t} \sin(\alpha x) \sin(\beta y) \\ X_{mn} e^{i\omega t} \sin(\alpha x) \sin(\beta y) \end{Bmatrix} \quad (21)$$

where  $\omega$  is the frequency of free vibration of FG plate,  $\sqrt{-1} = -1$  the imaginary unit. The coefficients  $\alpha$  and  $\beta$  are given by

$$\alpha = m\pi/a, \quad \beta = n\pi/b \quad (22)$$

The transverse load  $q$  is also expanded in the double-Fourier sine series as

Table 3 Non-dimensional stresses and displacements of Al<sub>2</sub>/AlO<sub>3</sub> square plates ( $a/h=10$ )

$p$	Theory	$\bar{u}(-h/4)$	$\bar{w}$	$\bar{\sigma}_x(h/3)$	$\bar{\sigma}_{xy}(-h/3)$	$\bar{\sigma}_{xz}(h/6)$
1	Quasi-3D (Carrera <i>et al.</i> 2008)	0.6436	0.5875	1.5062	0.6081	0.2510
	Quasi-3D (Wu <i>et al.</i> 2011)	0.6436	0.5876	1.5061	0.6112	0.2511
	SSDT (Zenkour, 2006)	0.6626	0.5889	1.4894	0.6110	0.2622
	HSDT (Mantari <i>et al.</i> 2012)	0.6398	0.5880	1.4888	0.6109	0.2566
	TSDT (Wu and Li, 2010)	0.6414	0.5890	1.4898	0.6111	0.2599
	TSDT (Thai and Kim, 2013)	0.6414	0.5890	1.4898	0.6111	0.2608
	Model 1	0.6407	0.5888	1.4891	0.611	0.2626
	Model 2	0.6410	0.5889	1.4894	0.6110	0.2621
2	Quasi-3D (Carrera <i>et al.</i> 2008)	0.9012	0.7570	1.4147	0.5421	0.2496
	Quasi-3D (Wu <i>et al.</i> 2011)	0.9013	0.7571	1.4133	0.5436	0.2495
	SSDT (Zenkour, 2006)	0.9281	0.7573	1.3954	0.5441	0.2763
	HSDT (Mantari <i>et al.</i> 2012)	0.8957	0.7564	1.3940	0.5438	0.2741
	TSDT (Wu and Li, 2010)	0.8984	0.7573	1.3960	0.5442	0.2721
	TSDT (Thai and Kim, 2013)	0.8984	0.7573	1.396	0.5442	0.2737
	Model 1	0.8972	0.7573	1.3949	0.544	0.2778
	Model 2	0.8977	0.7573	1.3954	0.5441	0.2763
4	Quasi-3D (Carrera <i>et al.</i> 2008)	1.0541	0.8823	1.1985	0.5666	0.2362
	Quasi-3D (Wu <i>et al.</i> 2011)	1.0541	0.8823	1.1841	0.5671	0.2362
	SSDT (Zenkour, 2006)	1.0941	0.8819	1.1783	0.5667	0.2580
	HSDT (Mantari <i>et al.</i> 2012)	1.0457	0.8814	1.1755	0.5662	0.2623
	TSDT (Wu and Li, 2010)	1.0502	0.8815	1.1794	0.5669	0.2519
	TSDT (Thai and Kim, 2013)	1.0502	0.8815	1.1794	0.5669	0.2537
	Model 1	1.0484	0.882	1.1774	0.5666	0.261
	Model 2	1.0492	0.8818	1.1783	0.5667	0.2580
8	Quasi-3D (Carrera <i>et al.</i> 2008)	1.0830	0.9738	0.9687	0.5879	0.2262
	Quasi-3D (Wu <i>et al.</i> 2011)	1.0830	0.9739	0.9622	0.5883	0.2261
	SSDT (Zenkour, 2006)	1.1340	0.9750	0.9466	0.5856	0.2121
	HSDT (Mantari <i>et al.</i> 2012)	1.0709	0.9737	0.9431	0.5850	0.2140
	TSDT (Wu and Li, 2010)	1.0763	0.9747	0.9477	0.5858	0.2087
	TSDT (Thai and Kim, 2013)	1.0763	0.9746	0.9477	0.5858	0.2088
	Model 1	1.0741	0.9751	0.9456	0.5854	0.2143
	Model 2	1.0751	0.9749	0.9466	0.5856	0.2121

$$q(x, y) = \sum_{m=1}^{\infty} \sum_{n=1}^{\infty} Q_{mn} \sin(\alpha x) \sin(\beta y) \quad (23)$$

where  $Q_{mn} = q_0$  for sinusoidally distributed load.

Substituting Eqs. (21) and (23) into Eq. (19), the following problem is obtained

$$\begin{bmatrix} S_{11} & S_{12} & S_{13} & S_{14} \\ S_{12} & S_{22} & S_{23} & S_{24} \\ S_{13} & S_{23} & S_{33} & S_{34} \\ S_{14} & S_{24} & S_{34} & S_{44} \end{bmatrix} - \omega^2 \begin{bmatrix} m_{11} & 0 & m_{13} & m_{14} \\ 0 & m_{22} & m_{23} & m_{24} \\ m_{13} & m_{23} & m_{33} & m_{34} \\ m_{14} & m_{24} & m_{34} & m_{44} \end{bmatrix} \begin{Bmatrix} U_{mn} \\ V_{mn} \\ W_{mn} \\ X_{mn} \end{Bmatrix} = \begin{Bmatrix} 0 \\ 0 \\ 0 \\ 0 \end{Bmatrix} \quad (24)$$

where

$$\begin{aligned} S_{11} &= -(\alpha^2 A_{11} + \beta^2 A_{66}), \quad S_{12} = -\alpha\beta(A_{12} + A_{66}), \\ S_{13} &= \alpha(\alpha^2 B_{11} - \beta^2(B_{12} + 2B_{66})), \\ S_{14} &= \alpha(k_1 B_{11}^s + k_2 B_{12}^s - (k_1 A' + k_2 B')\beta^2 B_{66}^s), \\ S_{22} &= -(\alpha^2 A_{66} + \beta^2 A_{22}), \end{aligned} \quad (25)$$

$$\begin{aligned} S_{23} &= \beta^3 B_{22} + \alpha^2 \beta(B_{12} + 2B_{66}), \\ S_{24} &= \beta(k_1 B_{22}^s + k_2 B_{12}^s - (k_1 A' + k_2 B')\alpha^2 B_{66}^s), \\ S_{33} &= -(\alpha^4 D_{11} + 2\alpha^2 \beta^2(D_{12} + 2D_{66}) + \beta^4 D_{22}), \\ S_{34} &= -k_1(\alpha^2 D_{11}^s + \beta^2 D_{12}^s) + 2(k_1 A' + k_2 B')\alpha^2 \beta^2 D_{66}^s - k_2(\beta^2 D_{22}^s + \alpha^2 D_{12}^s), \\ S_{44} &= -k_1(k_1 H_{11}^s + k_2 H_{12}^s) - (k_1 A' + k_2 B')^2 \alpha^2 \beta^2 H_{66}^s - k_2(k_1 H_{12}^s + k_2 H_{22}^s) \\ &\quad - (k_1 A')^2 \alpha^2 A_{55}^s - (k_2 B')^2 \beta^2 A_{44}^s \end{aligned} \quad (25)$$

$$m_{11} = -I_0, \quad m_{13} = \alpha I_1, \quad m_{14} = -k_1 A' \alpha J_1,$$

$$m_{22} = -I_0, \quad m_{23} = \beta I_1, \quad m_{24} = -k_2 B' \beta J_1$$

$$m_{33} = -I_0 - (\alpha^2 + \beta^2) I_2, \quad m_{34} = (k_1 A' \alpha^2 + k_2 B' \beta^2) J_2,$$

$$m_{44} = -K_2((k_1 A')^2 \alpha^2 + (k_2 B')^2 \beta^2)$$

#### 4. Numerical results

In this section, various numerical examples are examined and discussed to check the accuracy of the

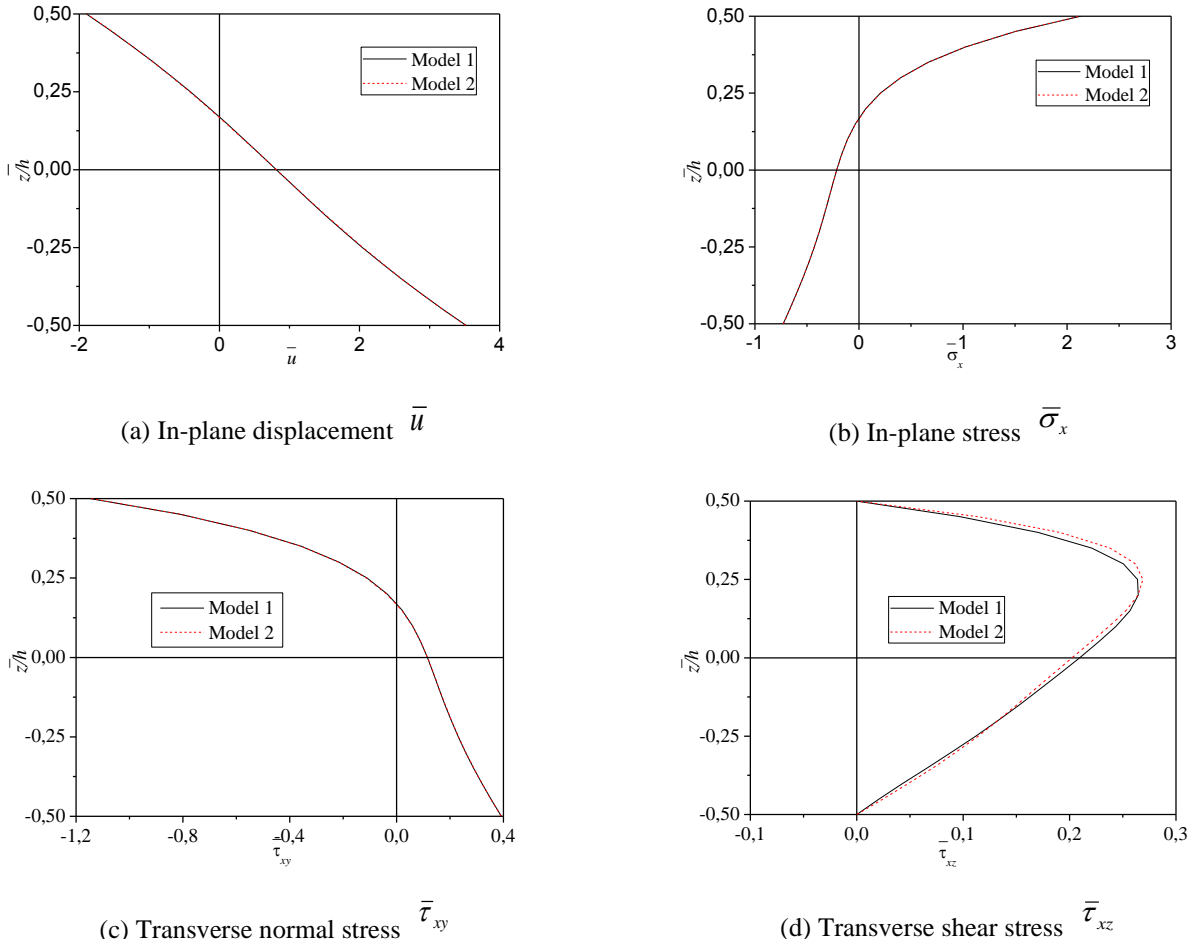


Fig. 2 Variation of non-dimensional displacement and stresses through the thickness of Al/Al<sub>2</sub>O<sub>3</sub> square plates ( $a/h=5, p=4$ )

proposed theory in predicting the bending and dynamic responses of simply supported FG plates. Two types of FGMs are studied: Al/Al<sub>2</sub>O<sub>3</sub> and Al/ZrO<sub>2</sub>. The material properties of FG plates are presented in Table 1. The Young's modulus and density of FG plates, unless mentioned otherwise, are calculated by employing the power law variation (see Eq. (7a)). For static investigation, a plate under sinusoidal load is considered. For convenience, the following dimensionless forms are employed

$$\begin{aligned} \bar{u} &= \frac{100E_c h^3}{q_0 a^4} u\left(0, \frac{b}{2}, z\right), & \bar{w} &= \frac{10E_c h^3}{q_0 a^4} w\left(\frac{a}{2}, \frac{b}{2}\right) \\ \bar{\sigma}_x(z) &= \frac{h}{q_0 a} \sigma_x\left(\frac{a}{2}, \frac{b}{2}, z\right), & \bar{\tau}_{xy}(z) &= \frac{h}{q_0 a} \tau_{xy}(0, 0, z) \\ \bar{\tau}_{xz}(z) &= \frac{h}{q_0 a} \tau_{xz}\left(0, \frac{b}{2}, z\right), & \hat{\omega} &= \omega h \sqrt{\rho_c/E_c}, & \bar{\omega} &= \frac{\omega a^2}{h} \sqrt{\rho_c/E_c} \\ \bar{\beta} &= \omega h \sqrt{\rho_m/E_m} \end{aligned} \quad (26)$$

#### 4.1 Bending investigation

**Example 1:** The first example is established for thin and thick Al/Al<sub>2</sub>O<sub>3</sub> square plates. Three different values of the gradient index  $p = 1, 4$  and  $10$  are taken into account. The

computed results are compared with quasi-3D solutions reported by Neves *et al.* (2012a, b and 2013) and Carrera *et al.* (2008, 2011) and those given by third shear deformation theory (TSDT) of Thai and Kim (2013), CPT (Carrera *et al.* 2008) and FSDT (Carrera *et al.* 2008). Table 2 presents non-dimensional normal stress  $\bar{\sigma}_x$  and vertical displacement  $\bar{w}$ . Noted that the studies of Neves *et al.* (2012a, b and 2013) and Carrera *et al.* (2008, 2011) are implemented via Carrera's unified formulation. However, the quasi-3D solutions of Neves *et al.* are obtained based on sinusoidal (Neves *et al.* 2012a), hyperbolic (Neves *et al.* 2012b), and cubic (Neves *et al.* 2013) distributions of in-plane displacement and a quadratic distribution of vertical displacement within the thickness, while the analytical (Carrera *et al.* 2008) and finite element (Carrera *et al.* 2011) quasi-3D solutions of Carrera *et al.* are determined based on fourth-order distributions of both in-plane and vertical displacement within the thickness. In addition, the quasi-3D solutions consider the thickness stretching influence (i.e.,  $\varepsilon_z \neq 0$ ), which is not introduced in FSDT and the two proposed models. It can be observed that the computed results are in good agreement with quasi-3D solutions particularly with those given by Neves *et al.* (2012b). In general, the two proposed models give a good prediction of both displacement and stress even in thick FG plates ( $a/h = 4$ )

Table 4 Non-dimensional vertical displacement  $\bar{w}$  of  $\text{Al}_2/\text{AlO}_3$  rectangular plates.

$a/h$	$b/a$	Theory	Gradient index ( $P$ )					
			0.1	0.3	0.5	0.7	1	1.5
1	1	3D (Zenkour, 2007)	0.5769	0.5247	0.4766	0.4324	0.3727	0.2890
		Quasi-3D (Zenkour, 2007)	0.5731	0.5181	0.4679	0.4222	0.3612	0.2771
		Quasi-3D (Mantari and Soares, 2012a)	0.5776	0.5222	0.4716	0.4255	0.3640	0.2792
		HSDT (Mantari and Soares, 2012b)	0.6363	0.5752	0.5195	0.4687	0.4018	0.3079
		TSDT (Thai and Kim, 2013)	0.6362	0.5751	0.5194	0.4687	0.4011	0.3079
		Model 1	0.6315	0.5709	0.5157	0.4654	0.3984	0.3061
		Model 2	0.6343	0.5734	0.5179	0.4674	0.3999	0.3072
		3D (Zenkour, 2007)	1.1944	1.0859	0.9864	0.8952	0.7727	0.6017
		Quasi-3D (Zenkour, 2007)	1.1880	1.0740	0.9701	0.8755	0.7494	0.5758
		Quasi-3D (Mantari and Soares, 2012a)	1.1938	1.0790	0.9748	0.8797	0.7530	0.5785
2	2	HSDT (Mantari and Soares, 2012b)	1.2776	1.1553	1.0441	0.9431	0.8093	0.6238
		TSDT (Thai and Kim, 2013)	1.2775	1.1553	1.0441	0.9431	0.8086	0.6238
		Model 1	1.2716	1.1500	1.0394	0.9389	0.8053	0.6216
		Model 2	1.2753	1.1532	1.0423	0.9415	0.8074	0.6231
		3D (Zenkour, 2007)	1.4430	1.3116	1.1913	1.0812	0.9334	0.7275
		Quasi-3D (Zenkour, 2007)	1.4354	1.2977	1.1722	1.0580	0.9057	0.6962
		Quasi-3D (Mantari and Soares, 2012a)	1.4419	1.3035	1.1774	1.0626	0.9096	0.6991
		HSDT (Mantari and Soares, 2012b)	1.5341	1.3874	1.2540	1.1329	0.9725	0.7506
		TSDT (Thai and Kim, 2013)	1.5340	1.3873	1.2540	1.1329	0.9719	0.7506
		Model 1	1.5277	1.3817	1.2490	1.1285	0.9684	0.7484
		Model 2	1.5316	1.3852	1.2521	1.1313	0.9706	0.7499
3	3	3D (Zenkour, 2007)	0.3490	0.3168	0.2875	0.2608	0.2253	0.1805
		Quasi-3D (Zenkour, 2007)	0.3475	0.3142	0.2839	0.2563	0.2196	0.1692
		Quasi-3D (Mantari and Soares, 2012a)	0.3486	0.3152	0.2848	0.2571	0.2203	0.1697
		HSDT (Mantari and Soares, 2012b)	0.3602	0.3259	0.2949	0.2668	0.2295	0.1785
		TSDT (Thai and Kim, 2013)	0.3602	0.3259	0.2949	0.2668	0.2295	0.1785
		Model 1	0.3595	0.3253	0.2943	0.2663	0.2292	0.1783
		Model 2	0.3599	0.3257	0.2947	0.2666	0.2294	0.1785
		3D (Zenkour, 2007)	0.8153	0.7395	0.6708	0.6085	0.5257	0.4120
		Quasi-3D (Zenkour, 2007)	0.8120	0.7343	0.6635	0.5992	0.5136	0.3962
		Quasi-3D (Mantari and Soares, 2012a)	0.8145	0.7365	0.6655	0.6009	0.5151	0.3973
4	2	HSDT (Mantari and Soares, 2012b)	0.8325	0.7534	0.6819	0.6173	0.5319	0.4150
		TSDT (Thai and Kim, 2013)	0.8325	0.7534	0.6819	0.6173	0.5319	0.4150
		Model 1	0.8315	0.7525	0.6812	0.6167	0.5314	0.4148
		Model 2	0.8321	0.7531	0.6817	0.6172	0.5318	0.4150
		3D (Zenkour, 2007)	1.0134	0.9190	0.8335	0.7561	0.6533	0.5121
		Quasi-3D (Zenkour, 2007)	1.0094	0.9127	0.8248	0.7449	0.6385	0.4927
		Quasi-3D (Mantari and Soares, 2012a)	1.0124	0.9155	0.8272	0.7470	0.6404	0.4941
		HSDT (Mantari and Soares, 2012b)	1.0325	0.9345	0.8459	0.7659	0.6601	0.5154
		TSDT (Thai and Kim, 2013)	1.0325	0.9345	0.8459	0.7659	0.6601	0.5154
		Model 1	1.0315	0.9335	0.8451	0.7652	0.6595	0.5151
		Model 2	1.0322	0.9342	0.8457	0.7657	0.6600	0.5154

where the influences of shear deformation are considerable. Whereas, the FSDT gives a good prediction of displacement only, but the stress is no better than those given by CPT. Noted that the two proposed models have only four

variables, while the number of variables in FSDT and quasi-3D (Neves *et al.* 2012b) is five and eleven, respectively. Also, the two proposed models do not required shear correction coefficients as in the case of FSDT.

Table 5 Non-dimensional fundamental frequencies  $\bar{\beta}$  of Al/ZrO<sub>3</sub> square FG plates

Theory	$p = 0$		$p = 1$			$a/h = 5$		
	$a/h = \sqrt{10}$	$a/h = 10$	$a/h = 5$	$a/h = 10$	$a/h = 20$	$p = 2$	$p = 3$	$p = 5$
3D (Vel and Batra, 2004)	0.4658	0.0596	0.2192	0.0578	0.0153	0.2211	0.2197	0.2225
Quasi-3D (Neves <i>et al.</i> 2012a)	—	—	0.2193	0.0596	0.0153	0.2198	0.2212	0.2225
Quasi-3D (Neves <i>et al.</i> 2012b)	—	—	0.2193	0.0596	0.0153	0.2201	0.2216	0.2230
Quasi-3D (Neves <i>et al.</i> 2013)	—	—	0.2193	—	—	0.2200	0.2215	0.2230
TSDT (Thai and Kim, 2013)	0.4623	0.0577	0.2169	0.0592	0.0152	0.2178	0.2193	0.2206
Model 1	0.4624	0.0577	0.2277	0.0619	0.0158	0.2257	0.2262	0.2271
Model 2	0.4628	0.0577	0.2277	0.0618	0.0158	0.2257	0.2262	0.2271

Table 6 non-dimensional frequency  $\bar{\omega}$  of Al/Al<sub>2</sub>O<sub>3</sub> square FG plates

$a/h$	Mode ( $m, n$ )	Theory	Gradient index ( $p$ )				
			0	0.5	1	4	10
5	1(1,1)	TSDT (Hosseini <i>et al.</i> 2011a)	0.2113	0.1807	0.1631	0.1378	0.1301
		FSDT (Hosseini <i>et al.</i> 2011b)	0.2112	0.1805	0.1631	0.1397	0.1324
		TSDT (Thai and Kim, 2013)	0.2113	0.1807	0.1631	0.1378	0.1301
		Model 1	0.2113	0.1807	0.1631	0.1377	0.1300
		Model 2	0.2113	0.1808	0.1632	0.1377	0.1300
	2(1,2)	TSDT (Hosseini <i>et al.</i> 2011a)	0.4623	0.3989	0.3607	0.2980	0.2771
		FSDT (Hosseini <i>et al.</i> 2011b)	0.4618	0.3978	0.3604	0.3049	0.2856
		TSDT (Thai and Kim, 2013)	0.4623	0.3989	0.3607	0.2980	0.2771
		Model 1	0.4624	0.3990	0.3608	0.2977	0.2770
		Model 2	0.4628	0.3992	0.3610	0.2976	0.2771
10	3(2,2)	TSDT (Hosseini <i>et al.</i> 2011a)	0.6688	0.5803	0.5254	0.4284	0.3948
		FSDT (Hosseini <i>et al.</i> 2011b)	0.6676	0.5779	0.5245	0.4405	0.4097
		TSDT (Thai and Kim, 2013)	0.6688	0.5803	0.5254	0.4284	0.3948
		Model 1	0.6693	0.5806	0.5257	0.4280	0.3948
		Model 2	0.6701	0.5812	0.5262	0.4280	0.3952
	2(1,2)	TSDT (Hosseini <i>et al.</i> 2011a)	0.0577	0.0490	0.0442	0.0381	0.0364
		FSDT (Hosseini <i>et al.</i> 2011b)	0.0577	0.0490	0.0442	0.0382	0.0366
		TSDT (Thai and Kim, 2013)	0.0577	0.0490	0.0442	0.0381	0.0364
		Model 1	0.0577	0.0490	0.0442	0.0381	0.0364
		Model 2	0.0577	0.0490	0.0442	0.0381	0.0364
20	1(1,1)	TSDT (Hosseini <i>et al.</i> 2011a)	0.1377	0.1174	0.1059	0.0903	0.0856
		FSDT (Hosseini <i>et al.</i> 2011b)	0.1376	0.1173	0.1059	0.0911	0.0867
		TSDT (Thai and Kim, 2013)	0.1377	0.1174	0.1059	0.0903	0.0856
		Model 1	0.1377	0.1174	0.1059	0.0902	0.0856
		Model 2	0.1377	0.1174	0.1059	0.0902	0.0856
	3(2,2)	TSDT (Hosseini <i>et al.</i> 2011a)	0.2113	0.1807	0.1631	0.1378	0.1301
		FSDT (Hosseini <i>et al.</i> 2011b)	0.2112	0.1805	0.1631	0.1397	0.1324
		TSDT (Thai and Kim, 2013)	0.2113	0.1807	0.1631	0.1378	0.1301
		Model 1	0.2113	0.1807	0.1631	0.1377	0.1300
		Model 2	0.2114	0.1808	0.1632	0.1377	0.1300

Table 7 The first two non-dimensional frequencies  $\bar{\omega}$  of  $Al/Al_2O_3$  square FG plates

Mode	$a/h$	Theory	Gradient index ( $p$ )				
			0	0.5	1	4	10
2	5	Quasi-3D (Matsunaga, 2008)	0.9400	0.8233	0.7477	0.5997	0.5460
		TSDT (Thai and Kim, 2013)	0.9297	0.8110	0.7356	0.5924	0.5412
		Model 1	0.9307	0.8118	0.7363	0.5921	0.5414
	10	Model 2	0.9323	0.8130	0.7374	0.5923	0.5423
		Quasi-3D (Matsunaga, 2008)	0.2121	0.1819	0.1640	0.1383	0.1306
		TSDT (Thai and Kim, 2013)	0.2113	0.1807	0.1631	0.1378	0.1301
1	5	Model 1	0.2113	0.1807	0.1631	0.1377	0.1300
		Model 2	0.2114	0.1808	0.1632	0.1377	0.1300
		Quasi-3D (Matsunaga, 2008)	0.0578	0.0492	0.0443	0.0381	0.0364
	10	TSDT (Thai and Kim, 2013)	0.0577	0.0490	0.0442	0.0381	0.0364
		Model 1	0.0577	0.0490	0.0442	0.0381	0.0364
		Model 2	0.0577	0.0490	0.0442	0.0380	0.0364
	2	Quasi-3D (Matsunaga, 2008)	1.7406	1.5425	1.4078	1.1040	0.9847
		TSDT (Thai and Kim, 2013)	1.7233	1.5192	1.3844	1.0919	0.9807
		Model 1	1.7283	1.5231	1.3880	1.0934	0.9836
		Model 2	1.7345	1.5279	1.3926	1.0963	0.9876
		Quasi-3D (Matsunaga, 2008)	0.4658	0.4040	0.3644	0.3000	0.2790
		TSDT (Thai and Kim, 2013)	0.4623	0.3989	0.3607	0.2980	0.2771
2	5	Model 1	0.4624	0.3990	0.3608	0.2977	0.2770
		Model 2	0.4628	0.3992	0.3610	0.2976	0.2771
		Quasi-3D (Matsunaga, 2008)	0.1381	0.1180	0.1063	0.0905	0.0859
	10	TSDT (Thai and Kim, 2013)	0.1376	0.1174	0.1059	0.0903	0.0856
		Model 1	0.1376	0.1174	0.1059	0.0902	0.0856
		Model 2	0.1376	0.1174	0.1059	0.0901	0.0856

**Example 2:** In the next example, a moderately thick  $Al/Al_2O_3$  square plate with  $a/h = 10$  is investigated. Table 3 shows non-dimensional displacements and stresses of plates for different values of gradient index  $p$ . The computed results are compared with the quasi-3D solutions reported by Carrera *et al.* (2008) and Wu *et al.* (2011) and those generated by the sinusoidal shear deformation theory (SSDT) (Zenkour, 2006), higher-order shear deformation theory (HSDT) (Mantari *et al.* 2012) and third-order shear deformation theory (TSDT) (Wu and Li, 2010, Thai and Kim, 2013). Since the influence of thickness stretching is omitted in 2D plate models (Zenkour, 2006, Mantari *et al.* 2012, Wu and Li, 2010, Thai and Kim, 2013) and the two proposed models, they lead to the solutions close to each other, and their solutions are also in good agreement with the quasi-3D solutions (Carrera *et al.* 2008, Wu *et al.* 2011). The through thickness variation for displacement and stresses are also presented and compared in Fig. 2 for a thick plate with  $a/h = 5$  and  $p = 4$ . In general, a good agreement between the results is observed, except in the case of the transverse shear stress  $\bar{\tau}_{xz}$  where a small difference between the results is found (see Fig. 2(d)).

**Example 3:** In this example, an  $Al/Al_2O_3$  plates with thickness ratios  $a/h = 2$  and 4 are investigated to check accuracy of the two proposed models for very thick FG

plates. The Young's modulus is calculated via the exponential distribution (Eq. 7b). The computed results are compared with 3D solutions (Zenkour, 2007), quasi-3D solutions (Zenkour, 2007, Mantari and Guedes Soares, 2012a), and those predicted by HSDT (Guedes Soares, 2012b) and TSDT (Thai and Kim, 2013) in Table 4. It

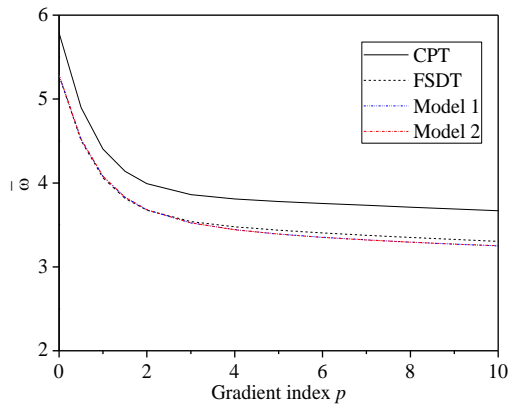


Fig. 3 Variation of non-dimensional fundamental natural frequency  $\bar{\omega}$  versus gradient index  $p$  of  $Al/Al_2O_3$  square FG plates ( $a/h = 5$ )

should be noted that the quasi-3D solutions reported by Zenkour (2007) are determined based on a sinusoidal distribution of both axial and vertical displacements, while the quasi-3D solutions provided by Mantari and Guedes Soares (2012a) are determined based on a cubic distribution of axial displacement and a quadratic distribution of vertical displacement. In general, the computed results are almost identical with those given by Mantari *et al.* (2012b) based on HSDT for all cases. Compared to 3D solutions (Zenkour, 2007) and quasi-3D solutions (Zenkour, 2007, Mantari and Guedes Soares, 2012a), the two proposed models slightly overestimate the vertical displacement of very thick FG plates with  $a/h = 2$ . This might be due to the thickness stretching influence in very thick plates which is neglected in the two proposed models, HSDT (Guedes Soares 2012b) and TSDT (Thai and Kim 2013). However, for thick plates with  $a/h = 4$ , good results are observed. It should be noted that the two proposed models contain four variables as against five in the case of HSDT (Mantari *et al.* 2012b) and six in the case of quasi-3D solutions (Zenkour 2007, Mantari and Guedes Soares 2012a). It can be concluded that the two proposed models are not only accurate but also efficient in predicting the responses of FG plates.

#### 4.1 Free vibration investigation

**Example 4:** In this example, a verification procedure is performed for thin and thick  $\text{Al}/\text{ZrO}_2$  square plates. The obtained results are compared with those generated with 3D solutions of Vel and Batra (2004), quasi-3D solutions of Neves *et al.* (2012a, b and 2013) and TSDT of Thai and Kim (2013). The Young's modulus is predicted via Mori-Tanaka scheme. The non-dimensional fundamental frequency  $\bar{\omega}$  is given in Table 5 for different values of thickness ratio and gradient index. It can be observed that the computed results agree well with the 3D solutions (Vel and Batra 2004) and quasi-3D solutions (Neves *et al.* 2012a, b and 2013).

**Example 5:** In the next example, thin and thick  $\text{Al}/\text{Al}_2\text{O}_3$  square plates with thickness ratio varied from 5 to 20 and gradient index varied from 0 to 10 are investigated using different plate models. The non-dimensional frequencies  $\bar{\omega}$  generated by TSDT (Hosseini-Hashemi *et al.* 2011a), FSDT (Hosseini-Hashemi *et al.* 2011b), TSDT (Thai and Kim, 2013), and the two proposed models are compared in Table 6. A good agreement between the results given by TSDT (Hosseini-Hashemi *et al.* 2011a) and the two proposed models is found for all modes of vibration. It should be noted that the TSDT (Hosseini-Hashemi *et al.* 2011a) contains more number of variables than the two proposed models. To further demonstrate the accuracy of the two proposed models for wide range of gradient index  $p$  and thickness ratio  $a/h$ , Figs. 3 and 4 illustrate the variation of non-dimensional frequency  $\bar{\omega}$  versus the gradient index  $p$  and thickness ratio  $a/h$ , respectively. It can be observed that the two proposed models generated almost identical results for all values of gradient index  $p$  (see Fig. 3) and thickness ratio  $a/h$  (see Fig. 4), whereas FSDT slightly overestimates the frequency of FG plates at high value of gradient index  $p$ . This is due to the employ of a constant

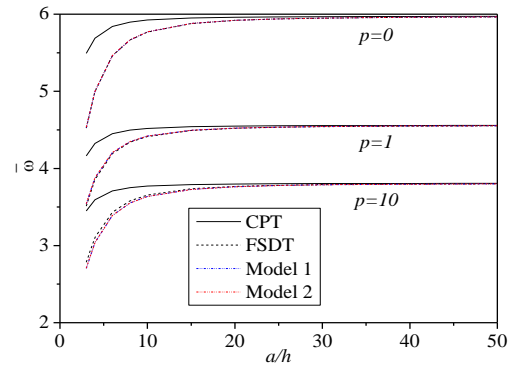


Fig. 4 Variation of non-dimensional fundamental natural frequency  $\bar{\omega}$  versus side-to-thickness ratio ( $a/h$ ) of  $\text{Al}/\text{Al}_2\text{O}_3$  square FG plates

shear correction coefficient for any values of gradient index  $p$ . Since CPT neglects the shear deformation influences, it overestimates frequency of thick plates (see Fig. 3).

**Example 6:** In the last example,  $\text{Al}/\text{Al}_2\text{O}_3$  square plates with thickness ratio  $a/h$  varied from 2 to 10 are examined. The aim of this example is to check the accuracy of the two proposed models for very thick FG plates. Table 7 presents the first two non-dimensional frequencies  $\hat{\omega}$  for various values of thickness ratio and gradient index. The obtained results are compared with those given by the quasi-3D theory (Matsunaga 2008) and TSDT (Thai and Kim 2013). Again, the computed results are shown to be in excellent agreement with quasi-3D solutions (Matsunaga 2008) for all modes of vibration even in very thick plates ( $a/h = 2$ ).

## 5. Conclusions

A simple HSDT for static and dynamic behaviors of FG plates is presented in this study. The theory accounts for the shear deformation influences without using a shear correction coefficient. By expressing the shear parts of the in-plane displacements with the integral term, the number of variables and governing equations of the two proposed models is reduced to four as against five in the FSDT and common HSDTs. Numerical results demonstrate that the two proposed models can be comparable with the existing HSDTs with a larger number of variables. An improvement of present approach will be considered in the future work to consider the thickness stretching effect by employing quasi-3D shear deformation models (Bessaim *et al.* 2013, Bousahla *et al.* 2014, Belabed *et al.* 2014, Fekrar *et al.* 2014, Hebali *et al.* 2014, Meradjah *et al.* 2015, Larbi Chaht *et al.* 2015, Hamidi *et al.* 2015, Bourada *et al.* 2015, Bennoun *et al.* 2016, Draiche *et al.* 2016, Benbakhti *et al.* 2016, Benahmed *et al.* 2017, Ait Atmane *et al.* 2017, Benchohra *et al.* 2017, Bouafia *et al.* 2017, ) and the wave propagation problem (Mahmoud *et al.* 2015, Ait Yahia *et al.* 2015, Boukhari *et al.* 2016, Meftah *et al.* 2017, Zaoui *et al.* 2017b).

## References

- Ait Atmane, H., Tounsi, A., Mechab, I., Adda Bedia, E.A. (2010), "Free vibration analysis of functionally graded plates resting on Winkler-Pasternak elastic foundations using a new shear deformation theory", *Int. J. Mech. Mater. Des.*, **6**(2), 113–121. <https://doi.org/10.1007/s10999-010-9110-x>
- Ait Atmane, H., Tounsi, A., Bernard, F. (2017), "Effect of thickness stretching and porosity on mechanical response of a functionally graded beams resting on elastic foundations", *Int. J. Mech. Mater. Des.*, **13**(1), 71 - 84. <https://doi.org/10.1007/s10999-015-9318-x>
- Ait Amar Meziane, M., Abdelaziz, H.H. and Tounsi, A. (2014), "An efficient and simple refined theory for buckling and free vibration of exponentially graded sandwich plates under various boundary conditions", *J. Sandw. Struct. Mater.*, **16**(3), 293-318. <https://doi.org/10.1177/1099636214526852>.
- Ait Yahia, S., Ait Atmane, H., Houari, M.S.A., Tounsi, A. (2015), "Wave propagation in functionally graded plates with porosities using various higher-order shear deformation plate theories", *Struct. Eng. Mech.*, **53**(6), 1143 – 1165. <https://doi.org/10.12989/sem.2015.53.6.1143>.
- Akavci, S.S. (2016), "Mechanical behavior of functionally graded sandwich plates on elastic foundation", *Compos. Part B*, **96**, 136 – 152. <https://doi.org/10.1016/j.compositesb.2016.04.035>.
- Akbaş, Ş.D. (2016), "Forced vibration responses of functionally graded viscoelastic beams under thermal environment", *Int. J. Innov. Res. Sci. Eng. Technol.*, **5**(12), 36 – 46.
- Aldousari, S.M. (2017), "Bending analysis of different material distributions of functionally graded beam", *Appl. Phys. A: Mater. Sci. Process.*, **123**(4), 296. <https://doi.org/10.1007/s00339-017-0854-0>
- Arani, A.J., Kolahchi, R. (2016), "Buckling analysis of embedded concrete columns armed with carbon nanotubes", *Comput. Concrete*, **17**(5), 567-578. <https://doi.org/10.12989/cac.2016.17.5.567>
- Baseri, V., Jafari, G.S., Kolahchi, R. (2016), "Analytical solution for buckling of embedded laminated plates based on higher order shear deformation plate theory", *Steel Compos. Struct.*, **21**(4), 883-919. <https://doi.org/10.12989/scs.2016.21.4.883>
- Belabed, Z., Houari, M.S.A., Tounsi, A., Mahmoud, S.R. and Anwar Bég, O. (2014), "An efficient and simple higher order shear and normal deformation theory for functionally graded material (FGM) plates", *Compos. Part B*, **60**, 274-283. <https://doi.org/10.1016/j.compositesb.2013.12.057>.
- Beldjelili, Y., Tounsi, A., & Mahmoud, S.R. (2016), "Hygro-thermo-mechanical bending of S-FGM plates resting on variable elastic foundations using a four-variable trigonometric plate theory", *Smart Struct. Syst.*, **18**(4), 755-786. <https://doi.org/10.12989/ss.2016.18.4.755>.
- Bellifa, H., Benrahou, K.H., Hadji, L., Houari, M.S.A. and Tounsi, A. (2016), "Bending and free vibration analysis of functionally graded plates using a simple shear deformation theory and the concept the neutral surface position", *J. Braz. Soc. Mech. Sci. Eng.*, **38**(1), 265-275. <https://doi.org/10.1007/s40430-015-0354-0>
- Benahmed, A., Houari, M.S.A., Benyoucef, S., Belakhdar, K., Tounsi, A. (2017), "A novel quasi-3D hyperbolic shear deformation theory for functionally graded thick rectangular plates on elastic foundation", *Geomech. Eng.*, **12**(1), 9-34. <https://doi.org/10.12989/gae.2017.12.1.009>
- Benbakhti, A., Bachir Bouiadja, M., Retiel, N., Tounsi, A. (2016), "A new five unknown quasi-3D type HSDT for thermomechanical bending analysis of FGM sandwich plates", *Steel Compos. Struct.*, **22**(5), 975 – 999. <https://doi.org/10.12989/scs.2016.22.5.975>
- Benchohra, M., Driz, H., Bakora, A., Tounsi, A., Adda Bedia, E.A., Mahmoud, S.R. (2017), "A new quasi-3D sinusoidal shear deformation theory for functionally graded plates", *Struct. Eng. Mech.*, **65**(1), 19-31. <https://doi.org/10.12989/SEM.2018.65.1.019>
- Bennoun, M., Houari, M.S.A. and Tounsi, A. (2016), "A novel five variable refined plate theory for vibration analysis of functionally graded sandwich plates", *Mech. Adv. Mater. Struct.*, **23**(4), 423-431. <https://doi.org/10.1080/15376494.2014.984088>
- Benveniste, Y. (1987), "A new approach to the application of Mori-Tanaka's theory in composite materials", *Mech. Mater.*, **6**(2), 147–157. [https://doi.org/10.1016/0167-6636\(87\)90005-6](https://doi.org/10.1016/0167-6636(87)90005-6)
- Benyoucef, S, Mechab, I, Tounsi, A, Fekrar, A, Ait Atmane, H, Adda Bedia, EA. (2010), "Bending of thick functionally graded plates resting on Winkler-Pasternak elastic foundations", *Mech. Compos. Mater.*, **46**(4), 425–434. <https://doi.org/10.1007/s11029-010-9159-5>.
- Bessaim, A., Houari, M.S.A., Tounsi, A., Mahmoud, S.R., Adda Bedia, E.A. (2013), "A new higher order shear and normal deformation theory for the static and free vibration analysis of sandwich plates with functionally graded isotropic face sheets", *J. Sandw. Struct. Mater.*, **15**, 671-703. <https://doi.org/10.1177/1099636213498888>
- Bilouei, B.S., Kolahchi, R., Bidgoli, M.R. (2016), "Buckling of concrete columns retrofitted with Nano-Fiber Reinforced Polymer (NFRP)", *Comput. Concrete*, **18**(5), 1053-1063. <https://doi.org/10.12989/cac.2016.18.5.1053>
- Birman, V., Byrd, LW. (2007), "Modeling and analysis of functionally graded materials and structures", *Appl. Mech. Rev.*, **60**, 195.
- Bouafia, K., Kaci, A., Houari, M.S.A., Benzair, A., Tounsi, A. (2017), "A nonlocal quasi-3D theory for bending and free flexural vibration behaviors of functionally graded nanobeams", *Smart Struct. Syst.*, **19**(2), 115-126. <https://doi.org/10.12989/ss.2017.19.2.115>
- Bouderba, B., Houari, M.S.A. and Tounsi, A. (2013) "Thermomechanical bending response of FGM thick plates resting on Winkler-Pasternak elastic foundations", *Steel Compos. Struct.*, **14**(1), 85-104. <https://doi.org/10.12989/scs.2013.14.1.085>
- Bouderba, B., Houari, M.S.A. and Tounsi, A. and Mahmoud, S.R. (2016), "Thermal stability of functionally graded sandwich plates using a simple shear deformation theory", *Struct. Eng. Mech.*, **58**(3), 397-422. <https://doi.org/10.12989/sem.2016.58.3.397>.
- Boukhari, A., Ait Atmane, H., Tounsi, A., Adda Bedia, E.A. and Mahmoud, S.R. (2016), "An efficient shear deformation theory for wave propagation of functionally graded material plates", *Struct. Eng. Mech.*, **57**(5), 837-859. <https://doi.org/10.12989/sem.2016.57.5.837>.
- Bourada, M., Kaci, A., Houari, M.S.A. and Tounsi, A. (2015), "A new simple shear and normal deformations theory for functionally graded beams", *Steel Compos. Struct.*, **18**(2), 409-423. <https://doi.org/10.12989/scs.2015.18.2.409>.
- Bousahla, A.A., Houari, M.S.A., Tounsi, A. and Adda Bedia, E.A. (2014), "A novel higher order shear and normal deformation theory based on neutral surface position for bending analysis of advanced composite plates", *Int. J. Comput. Meth.*, **11**(6), 1350082. <https://doi.org/10.1142/S0219876213500825>
- Bousahla, A.A., Benyoucef, S., Tounsi, A. and Mahmoud, S.R. (2016), "On thermal stability of plates with functionally graded coefficient of thermal expansion", *Struct. Eng. Mech.*, **60**(2), 313-335. <https://doi.org/10.12989/sem.2016.60.2.313>.
- Carrera, E., Brischetto, S., Robaldo, A. (2008), "Variable kinematic model for the analysis of functionally graded material plates", *AIAA J.*, **46**(1), 194–203. <https://doi.org/10.2514/1.32490>
- Carrera, E., Brischetto, S., Cinefra, M., Soave, M. (2011), "Effects of thickness stretching in functionally graded plates and shells", *Compos. Part B*, **42**(2), 123–133. <https://doi.org/10.1016/j.compositesb.2010.11.030>

- j.compositesb.2010.10.005
- Chaabane, L.A., Bourada, F., Sekkal, M., Zerouati, S., Zaoui, F.Z., Tounsi, A., Derras, A., Bousahla, A.A., Tounsi, A. (2019), "Analytical study of bending and free vibration responses of functionally graded beams resting on elastic foundation", *Struct. Eng. Mech.*, **71**(2), 185-196. <https://doi.org/10.12989/sem.2019.71.2.185>
- Chen, CS, Hsu, CY, Tzou, GJ. (2009), "Vibration and stability of functionally graded plates based on a higher-order deformation theory", *J. Reinf. Plast. Compos.*, **28**(10), 1215-1234. <https://doi.org/10.1177/0731684408088884>
- Draiche, K., Tounsi, A., Mahmoud, S.R. (2016), "A refined theory with stretching effect for the flexure analysis of laminated composite plates", *Geomech. Eng.*, **11**(5), 671-690. <https://doi.org/10.12989/gae.2016.11.5.671>
- Ebrahimi, F., Rastgoo, A. and Atai, A.A. (2009a), "A theoretical analysis of smart moderately thick shear deformable annular functionally graded plate", *Eur. J. Mech. A/Solids*, **28**(5), 962-973. <https://doi.org/10.1016/j.euromechsol.2008.12.008>
- Ebrahimi, F., Naei, M.H. and Rastgoo, A. (2009b), "Geometrically nonlinear vibration analysis of piezoelectrically actuated FGM plate with an initial large deformation", *J. mech. sci. technol.*, **23**(8), 2107-2124. <https://doi.org/10.1007/s12206-009-0358-8>
- Eltaher, M.A., Alshorbagy, A.E., Mahmoud, F.F. (2013), "Determination of neutral axis position and its effect on natural frequencies of functionally graded macro/nanobeams", *Compos. Struct.*, **99**, 193-201. <https://doi.org/10.1016/j.compstruct.2012.11.039>
- Fekrar, A., Houari, M.S.A., Tounsi, A., Mahmoud, S.R. (2014), "A new five-unknown refined theory based on neutral surface position for bending analysis of exponential graded plates", *Meccanica*, **49**, 795-810. <https://doi.org/10.1007/s11012-013-9827-3>
- Guerroudj, H.Z., Yeghnem, R., Kaci, A., Zaoui, F.Z., Benyoucef, S., Tounsi, A. (2018), "Eigenfrequencies of advanced composite plates using an efficient hybrid quasi-3D shear deformation theory", *Smart Struct. Syst.*, **22**(1), 121-132. <https://doi.org/10.12989/ss.2018.22.1.121>
- Hamidi, A., Houari, M.S.A., Mahmoud, S.R. and Tounsi, A. (2015), "A sinusoidal plate theory with 5-unknowns and stretching effect for thermomechanical bending of functionally graded sandwich plates", *Steel Compos. Struct.*, **18**(1), 235-253. <https://doi.org/10.12989/scs.2015.18.1.235>
- Hebali, H., Tounsi, A., Houari, M.S.A., Bessaim, A. and Adda Bedia, E.A. (2014), "A new quasi-3D hyperbolic shear deformation theory for the static and free vibration analysis of functionally graded plates", *J. Eng. Mech. ASCE*, **140**, 374-383. [https://doi.org/10.1061/\(ASCE\)EM.1943-7889.0000665](https://doi.org/10.1061/(ASCE)EM.1943-7889.0000665)
- Hosseini-Hashemi, S., Fadaee, M., Atashipour, SR. (2011a), "Study on the free vibration of thick functionally graded rectangular plates according to a new exact closed form procedure", *Compos. Struct.*, **93**(2), 722-735. <https://doi.org/10.1016/j.compstruct.2010.08.007>
- Hosseini-Hashemi, S., Fadaee, M., Atashipour, SR. (2011b), "A new exact analytical approach for free vibration of Reissner-Mindlin functionally graded rectangular plates", *Int. J. Mech. Sci.*, **53**(1), 11-22. <https://doi.org/10.1016/j.ijmecsci.2010.10.002>
- Kar, V.R., Panda, S.K., Mahapatra, T.R. (2016a), "Thermal buckling behaviour of shear deformable functionally graded single/doubly curved shell panel with TD and TID properties", *Adv. Mater. Res.*, **5**(4), 205-221. <https://doi.org/10.12989/amr.2016.5.4.205>
- Kar, V.R., Mahapatra, T.R., Panda, S.K. (2016b), "Effect of different temperature load on thermal postbuckling behaviour of functionally graded shallow curved shell panels", *Compos. Struct.*, **160**(15), 1236-1247. <https://doi.org/10.1016/j.compstruct.2016.10.125>
- Kar, V.R., Mahapatra, T.R., Panda, S.K. (2015), "Nonlinear flexural analysis of laminated composite flat panel under hydro-thermo-mechanical loading", *Steel Compos. Struct.*, **19**(4), 1011-1033. <https://doi.org/10.12989/scs.2015.18.3.693>
- Kitipornchai, S., Yang, J., Liew, KM. (2006), "Random vibration of the functionally graded laminates in thermal environments", *Comput. Methods Appl. Mech. Eng.*, **195**(9-12), 1075-1095. <https://doi.org/10.1016/j.cma.2005.01.016>
- Kolahchi, R. (2017), "A comparative study on the bending, vibration and buckling of viscoelastic sandwich nano-plates based on different nonlocal theories using DC, HDQ and DQ methods", *Aerospace Sci. Technol.*, **66**, 235-248. <https://doi.org/10.1016/j.ast.2017.03.016>
- Kolahchi, R., Hosseini, H., Esmailpour, M. (2016a), "Differential cubature and quadrature-Bolotin methods for dynamic stability of embedded piezoelectric nanoplates based on visco-nonlocal-piezoelasticity theories", *Compos. Struct.*, **157**, 174-186. <https://doi.org/10.1016/j.compstruct.2016.08.032>
- Kolahchi, R., Moniri Bidgoli, A.M. (2016), "Size-dependent sinusoidal beam model for dynamic instability of single-walled carbon nanotubes", *Appl. Math. Mech. -Engl. Ed.*, **37**(2), 265-274. <https://doi.org/10.1007/s10483-016-2030-8>
- Kolahchi, R., Safari, M., Esmailpour, M. (2016b), "Dynamic stability analysis of temperature-dependent functionally graded CNT-reinforced visco-plates resting on orthotropic elastomeric medium", *Compos. Struct.*, **150**, 255-265. <https://doi.org/10.1016/j.compstruct.2016.05.023>
- Kolahchi, R., Zarei, M.S., Hajmohammad, M.H., Oskouei, A.N. (2017a), "Visco-nonlocal-refined Zigzag theories for dynamic buckling of laminated nanoplates using differential cubature-Bolotin methods", *Thin-Wall. Struct.*, **113**, 162-169. <https://doi.org/10.1016/j.tws.2017.01.016>
- Kolahchi, R., Zarei, M.S., Hajmohammad, M.H., Nouri, A. (2017b), "Wave propagation of embedded viscoelastic FG-CNT-reinforced sandwich plates integrated with sensor and actuator based on refined zigzag theory", *Int. J. Mech. Sci.*, **130**, 534-545. <https://doi.org/10.1016/j.ijmecsci.2017.06.039>
- Larbi Chaht, F., Kaci, A., Houari, M.S.A., Tounsi, A., Anwar Bég, O., Mahmoud, S.R. (2015), "Bending and buckling analyses of functionally graded material (FGM) size-dependent nanoscale beams including the thickness stretching effect", *Steel Compos. Struct.*, **18**(2), 425-442. <https://doi.org/10.12989/scs.2015.18.2.425>
- Madani, H., Hosseini, H., Shokravi, M. (2016), "Differential cubature method for vibration analysis of embedded FG-CNT-reinforced piezoelectric cylindrical shells subjected to uniform and non-uniform temperature distributions", *Steel Compos. Struct.*, **22**(4), 889-913. <https://doi.org/10.12989/scs.2016.22.4.889>
- Mahapatra, T.R., Kar, V.R., Panda, S.K., Mehar, K. (2017), "Nonlinear thermoelastic deflection of temperature-dependent FGM curved shallow shell under nonlinear thermal loading", *J. Therm. Stresses*, **40**(9), 1184-1199. <https://doi.org/10.1080/01495739.2017.1302788>
- Mahapatra, T.R., Kar, V.R., Panda, S.K. (2016a), "Large amplitude vibration analysis of laminated composite spherical panels under hydrothermal environment", *Int. J. Struct. Stab. Dyn.*, **16**(3), 1450105. <https://doi.org/10.1142/S0219455414501053>
- Mahapatra, T.R., Panda, S.K., Kar, V.R. (2016b), "Nonlinear hygro-thermo-elastic vibration analysis of doubly curved composite shell panel using finite element micromechanical model", *Mech. Advanced Mater. Struct.*, **23**(11), 1343-1359. <https://doi.org/10.1142/S0219455414501053>
- Mahapatra, T.R., Kar, V.R., Panda, S.K. (2016c), "Large amplitude bending behaviour of laminated composite curved panels", *Eng. Comput.*, **33**(1), 116-138. <https://doi.org/10.1108/EC-05-2014-002>

- 0119
- Mahapatra, T.R., Panda, S.K., Kar, V.R. (2016d), "Nonlinear flexural analysis of laminated composite panel under hygro-thermo-mechanical loading — A micromechanical approach", *Int. J. Comput. Method.*, **33**(1), 116-138. <https://doi.org/10.1142/S0219876216500158>
- Mahapatra, T.R., Panda, S.K., Kar, V.R. (2016e), "Geometrically nonlinear flexural analysis of hygrothermo-elastic laminated composite doubly curved shell panel", *Int. J. Mech. Mater. Des.*, **12**(2), 153-171. <https://doi.org/10.1007/s10999-015-9299-9>
- Mahapatra, T.R., Panda, S.K. (2016), "Nonlinear free vibration analysis of laminated composite spherical shell panel under elevated hygrothermal environment: A micromechanical approach", *Aerosp. Sci. Technol.*, **49**, 276–288. <https://doi.org/10.1016/j.ast.2015.12.018>
- Mahapatra, T.R., Kar, V.R., Panda, S.K. (2015), "Nonlinear free vibration analysis of laminated composite doubly curved shell panel in hygrothermal environment", *J. Sandw. Struct. Mater.*, **17**(5), 511-545. <https://doi.org/10.1177/1099636215577363>
- Mahapatra, T.R., Panda, S.K. (2015), "Thermoelastic vibration analysis of laminated doubly curved shallow panels using nonlinear FEM", *J. Therm. Stresses*, **38**(1), 39-68. <https://doi.org/10.1080/01495739.2014.976125>
- Mahi, A., Adda Bedia, E.A. and Tounsi, A. (2015), "A new hyperbolic shear deformation theory for bending and free vibration analysis of isotropic, functionally graded, sandwich and laminated composite plates", *Appl. Math. Model.*, **39**, 2489-2508. <https://doi.org/10.1016/j.apm.2014.10.045>
- Mahmoud, SR, Abd-Alla, AM, Tounsi, A., Marin, M. (2015), "The problem of wave propagation in magneto-rotating orthotropic non-homogeneous medium", *J. Vib. Control*, **21**(16), 3281-3291. <https://doi.org/10.1177/1077546314521443>
- Mantari, JL, Oktem, AS, Guedes Soares, C. (2012), "Bending response of functionally graded plates by using a new higher order shear deformation theory", *Compos. Struct.*, **94**(2), 714–723. <https://doi.org/10.1016/j.compstruct.2011.09.007>
- Mantari, JL, Guedes Soares, C. (2012a), "Generalized hybrid quasi-3D shear deformation theory for the static analysis of advanced composite plates", *Compos. Struct.*, **94**(8), 2561–2575. <https://doi.org/10.1016/j.compstruct.2012.02.019>
- Mantari, JL, Guedes Soares, C. (2012b), "Bending analysis of thick exponentially graded plates using a new trigonometric higher order shear deformation theory", *Compos. Struct.*, **94**(6), 1991–2000. <https://doi.org/10.1016/j.compstruct.2012.01.005>
- Matsunaga, H. (2008), "Free vibration and stability of functionally graded plates according to a 2-D higher-order deformation theory", *Compos. Struct.*, **82**(4), 499–512. <https://doi.org/10.1016/j.compstruct.2007.01.030>
- Meftah, A., Bakora, A., Zaoui, F.Z., Tounsi, A. and Adda Bedia, E.A. (2017), "A non-polynomial four variable refined plate theory for free vibration of functionally graded thick rectangular plates on elastic foundation", *Steel Compos. Struct.*, **23**(3), 317-330. <https://doi.org/10.12989/scs.2017.23.3.317>
- Mehar, K., Panda, S.K. (2017), "Thermoelastic nonlinear frequency analysis of CNT reinforced functionally graded sandwich structure", *Eur. J. Mech. -A/Solids*, **65**, 384-396. <https://doi.org/10.1016/j.euromechsol.2017.05.005>
- Meksi, A., Benyoucef, S., Houari, M.S.A. and Tounsi, A. (2015), "A simple shear deformation theory based on neutral surface position for functionally graded plates resting on Pasternak elastic foundations", *Struct. Eng. Mech.*, **53**(6), 1215-1240. <https://doi.org/10.12989/sem.2015.53.6.1215>
- Meradjah, M., Kaci, A., Houari, M.S.A., Tounsi, A., Mahmoud, S.R. (2015), "A new higher order shear and normal deformation theory for functionally graded beams", *Steel Compos. Struct.*, **18**(3), 793-809. <https://doi.org/10.12989/scs.2015.18.3.793>
- Meradjah, M., Bouakkaz, K., Zaoui, F.Z., Tounsi, A. (2018), "A refined quasi-3D hybrid-type higher order shear deformation theory for bending and Free vibration analysis of advanced composites beams", *Wind Struct.*, **27**(4), 269-282. <https://doi.org/10.12989/was.2018.27.4.269>
- Mindlin, R.D. (1951), "Influence of rotatory inertia and shear on flexural motions of isotropic, elastic plates", *ASME J. Appl. Mech.*, **18**, 31-38.
- Mori, T, Tanaka, K. (1973), "Average stress in matrix and average elastic energy of materials with misfitting inclusions", *Acta Metall.*, **21**(5), 571-574. [https://doi.org/10.1016/0001-6160\(73\)90064-3](https://doi.org/10.1016/0001-6160(73)90064-3)
- Neves, AMA, Ferreira, AJM, Carrera, E, Roque, CMC, Cinefra, M, Jorge, RMN, et al. (2012a), "A quasi-3D sinusoidal shear deformation theory for the static and free vibration analysis of functionally graded plates", *Compos. Part B*, **43**(2), 711–725. <https://doi.org/10.1016/j.compositesb.2011.08.009>
- Neves, AMA, Ferreira, AJM, Carrera, E, Cinefra, M, Roque, CMC, Jorge, RMN, et al. (2012b), "A quasi-3D hyperbolic shear deformation theory for the static and free vibration analysis of functionally graded plates", *Compos. Struct.*, **94**(5), 1814–1825. <https://doi.org/10.1016/j.compstruct.2011.12.005>
- Neves, AMA, Ferreira, AJM, Carrera, E, Cinefra, M, Roque, CMC, Jorge, RMN, et al. (2013), "Static, free vibration and buckling analysis of isotropic and sandwich functionally graded plates using a quasi-3D higher-order shear deformation theory and a meshless technique", *Compos. Part B*, **44**(1), 657 - 674. <https://doi.org/10.1016/j.compositesb.2012.01.089>
- Pradyumna, S, Bandyopadhyay, JN. (2008), "Free vibration analysis of functionally graded curved panels using a higher-order finite element formulation", *J. Sound Vib.*, **318**(1-2), 176–192. <https://doi.org/10.1016/j.jsv.2008.03.056>
- Rahmani, O., Refaeinejad, V., Hosseini, S.A.H. (2017), "Assessment of various nonlocal higher order theories for the bending and buckling behavior of functionally graded nanobeams", *Steel Compos. Struct.*, **23**(3), 339-350. <https://doi.org/10.12989/scs.2017.23.3.339>
- Raminneha, M., Biglari, H., Vakili Tahami, F. (2016), "Nonlinear higher order Reddy theory for temperature- dependent vibration and instability of embedded functionally graded pipes conveying fluid-nanoparticle mixture", *Struct. Eng. Mech.*, **59**(1), 153-186. <https://doi.org/10.12989/sem.2016.59.1.153>
- Reddy, J.N. (2000), "Analysis of functionally graded plates", *Int. J. Numer. Methods Eng.*, **47**(1-3), 663–684. [https://doi.org/10.1002/\(SICI\)1097-0207\(20000110/30\)47:1/3<663::AID-NME787>3.0.CO;2-8](https://doi.org/10.1002/(SICI)1097-0207(20000110/30)47:1/3<663::AID-NME787>3.0.CO;2-8)
- Reddy, J.N. (2011), "A general nonlinear third-order theory of functionally graded plates", *Int. J. Aerosp. Lightw. Struct.*, **1**(1), 1–21. <https://doi.org/10.3850/S201042861100002X>
- Sahoo, S.S., Pand, S.K., Mahapatra, T.R. (2016), "Static, free vibration and transient response of laminated composite curved shallow panel – An experimental approach", *Eur. J. Mech. -A/Solids*, **59**, 95-113. <https://doi.org/10.1016/j.euromechsol.2016.03.014>
- Swaminathan, K. and Naveenkumar, D.T. (2014), "Higher order refined computational models for the stability analysis of FGM plates: Analytical solutions", *Eur. J. Mech. A/Solid.*, **47**, 349 - 361. <https://doi.org/10.1016/j.euromechsol.2014.06.003>
- Talha, M, Singh, BN. (2010), "Static response and free vibration analysis of FGM plates using higher order shear deformation theory", *Appl. Math. Model.*, **34**(12), 3991–4011. <https://doi.org/10.1016/j.apm.2010.03.034>
- Thai, H.T, Kim, S.E. (2013), "A simple higher-order shear deformation theory for bending and free vibration analysis of functionally graded plates", *Compos. Struct.*, **96**, 165–173. <https://doi.org/10.1016/j.compstruct.2012.08.025>
- Tounsi, A., Houari, M.S.A., Benyoucef, S. and Adda Bedia, E.A. (2013), "A refined trigonometric shear deformation theory for

- thermoelastic bending of functionally graded sandwich plates”, *Aerosp. Sci. Tech.*, **24**, 209-220. <https://doi.org/10.1016/j.ast.2011.11.009>
- Vel, SS, Batra, RC. (2004), “Three-dimensional exact solution for the vibration of functionally graded rectangular plates”, *J. Sound Vib.*, **272**(3–5), 703–730. [https://doi.org/10.1016/S0022-460X\(03\)00412-7](https://doi.org/10.1016/S0022-460X(03)00412-7)
- Wu, CP, Chiu, KH, Wang, YM. (2011), “RMVT-based meshless collocation and elementfree Galerkin methods for the quasi-3D analysis of multilayered composite and FGM plates”, *Compos. Struct.*, **93**(2), 923–943. <https://doi.org/10.1016/j.compstruct.2010.11.015>
- Wu, CP, Li, HY. (2010), “An RMVT-based third-order shear deformation theory of multilayered functionally graded material plates”, *Compos. Struct.*, **92**(10), 2591–2605. <https://doi.org/10.1016/j.compstruct.2010.01.022>
- Xiang, S, Jin, YX, Bi, ZY, Jiang, SX, Yang, MS. (2011), “A n-order shear deformation theory for free vibration of functionally graded and composite sandwich plates”, *Compos. Struct.*, **93**(11), 2826–2832. <https://doi.org/10.1016/j.compstruct.2011.05.022>
- Yang, J, Liew, KM, Kitipornchai, S. (2005), “Stochastic analysis of compositionally graded plates with system randomness under static loading”, *Int. J. Mech. Sci.*, **47**(10), 1519–1541. <https://doi.org/10.1016/j.ijmecsci.2005.06.006>
- Younsi, A., Tounsi, A., Zaoui, F.Z., Bousahla, A.A., Mahmoud S.R. (2018), “Novel quasi-3D and 2D shear deformation theories for bending and free vibration analysis of FGM plates”, *Geomech. Eng.*, **14**(6), 519-532. <https://doi.org/10.12989/gae.2018.14.6.519>
- Zamanian, M., Kolahchi, R., Bidgoli, M.R. (2017), “Agglomeration effects on the buckling behavior of embedded concrete columns reinforced with SiO<sub>2</sub> nano-particles”, *Wind Struct.*, **24**(1), 43-57. <https://doi.org/10.12989/was.2017.24.1.043>
- Zaoui, F.Z., Hanifi Hachemi Amar, L., Younsi A., Meradjah M., Tounsi, A., and Ouinas, Dj. (2017a), “Free vibration analysis of functionally graded beams using a higher-order shear deformation theory”, *Math. Model. Eng. Problems*, **4**(1):7-12. <https://doi.org/10.18280/mmep.040102>
- Zaoui, F.Z., Tounsi, A., and Ouinas, Dj. (2017b), “Free vibration of functionally graded plates resting on elastic foundations based on quasi-3D hybrid-type higher order shear deformation theory”, *Smart Struct. Syst.*, **20**(4): 509-524. <https://doi.org/10.12989/ssss.2017.20.4.509>
- Zaoui, F.Z., Ouinas, D., Tounsi, A. (2019), “New 2D and quasi-3D shear deformation theories for free vibration of functionally graded plates on elastic foundations”, *Compos. Part B*, **159**, 231-247. <https://doi.org/10.1016/j.compositesb.2018.09.051>
- Zemri, A., Houari, M.S.A., Bousahla, A.A. and Tounsi, A. (2015), “A mechanical response of functionally graded nanoscale beam: an assessment of a refined nonlocal shear deformation theory beam theory”, *Struct. Eng. Mech.*, **54**(4), 693-710. <https://doi.org/10.12989/sem.2015.54.4.693>
- Zenkour, AM. (2006), “Generalized shear deformation theory for bending analysis of functionally graded plates”, *Appl. Math. Model.*, **30**(1), 67–84. <https://doi.org/10.1016/j.apm.2005.03.009>
- Zenkour, AM. (2007), “Benchmark trigonometric and 3-D elasticity solutions for an exponentially graded thick rectangular plate”, *Arch. Appl. Mech.*, **77**(4), 197–214. <https://doi.org/10.1007/s00419-006-0084-y>
- Zidi, M., Tounsi, A., Houari, M.S.A., Adda Bedia, E.A. and Anwar Bég, O. (2014), “Bending analysis of FGM plates under hydro-thermo-mechanical loading using a four variable refined plate theory”, *Aerosp. Sci. Technol.*, **34**, 24-34. <https://doi.org/10.1016/j.ast.2014.02.001>
- Zidi, M., Houari, M.S.A., Tounsi, A., Bessaim, A., Mahmoud, S.R. (2017), “A novel simple two-unknown hyperbolic shear deformation theory for functionally graded beams”, *Struct. Eng. Mech.*, **64**(2), 145-153. <https://doi.org/10.12989/sem.2017.64.2.145>

CC